

A LAYERED AQUIFER MODEL OF ATOLL ISLAND
HYDROLOGY: VALIDATION OF A COMPUTER SIMULATION


M. E. HERMAN
R. W. BUDDEMEIER
S. W. WHEATCRAFT

THIS PAPER WAS PREPARED FOR SUBMITTAL
TO THE JOURNAL OF HYDROLOGY

JULY 3, 1985



Lawrence
Livermore
National
Laboratory



This is a preprint of a paper intended for publication in a journal or proceedings. Since changes may be made before publication, this preprint is made available with the understanding that it will not be cited or reproduced without the permission of the author.

A LAYERED AQUIFER MODEL OF ATOLL ISLAND HYDROLOGY:
VALIDATION OF A COMPUTER SIMULATION

M. E. HERMAN

Desert Research Institute, University of Nevada System, P.O. Box 60220, Reno,
NV 89506 (USA) [present address: U.S. Environmental Protection Agency, 8WM-DW,
999 18th Street, Denver, CO 90202 (USA)]

R. W. BUDDEMEIER

Lawrence Livermore National Laboratory, P.O. Box 808, Livermore, CA 94550
(USA)

S. W. WHEATCRAFT

Desert Research Institute, University of Nevada System, P.O. Box 60220, Reno,
NV 89506 (USA)

ABSTRACT

The finite-element model FEMWATER was used to simulate groundwater movement in the two-dimensional vertical plane of an atoll island section. The model island had dimensions consistent with Enjebi Island (Enewetak Atoll), a surficial (Holocene) aquifer to a depth of 15 m with hydraulic conductivity = 6.0×10^{-4} m/sec, overlying a (Plio-Pleistocene) aquifer with $K = 6.0 \times 10^{-2}$ m/sec. A tidally varying water level was applied to the ocean and lagoon boundaries, and the model was run until pseudo steady-state conditions were achieved in the groundwater variations. Hydraulic head contours in the vertical section demonstrate that water motion under the supratidal portion of the island is almost exclusively vertical. Calculated water table tidal lags and efficiencies are in excellent agreement with measured values from shallow wells on Enjebi Island, confirming the validity of the layered aquifer model and the approximate magnitudes of the hydraulic conductivities. Model results near island margins can be interpreted to explain other features of hydrologic field data from atoll islands. The results emphasize the potential importance of tidal effects and vertical water flow on reef island groundwater systems, and cast doubt on the utility of traditional models using the Ghyben-Herzberg lens concept modeled on the basis

of the Dupuit assumptions.

1. INTRODUCTION

Quantitative models of atoll island hydrology are of interest and utility from several standpoints. The "low islands" of the Pacific are recent carbonate sedimentary structures perched atop oceanic coral reefs. There is considerable scientific interest in coral reef systems, both in terms of present structure and function and in relation to their development and diagenesis over time. An understanding of water movement through and within these structures, and particularly of the distribution of fresh water in the island ground-water systems, would be relevant to a wide variety of disciplines. On a more practical level, the inhabitants of many such islands rely on ground water as a primary or backup source of fresh water for domestic and agricultural use. An accurate hydrologic model is essential to effective resource evaluation and exploitation on islands which are often characterized by limited extent, variable rainfall and increasing population.

The conceptual basis for most island and coastal models is the Ghyben-Herzberg principle. In its most basic form, this is simply the observation that fresh-water recharge to an oceanic island will tend, when restrained and protected from wave and tidal mixing by the porous medium, to form a lens of fresh water which floats upon the underlying seawater in the formation. The head induced by this fresh-water lens is related to the total thickness of the fresh-water lens and the density difference between sea water and fresh water; typically, one unit of head elevation above mean sea level (MSL) indicates the presence of an idealized fresh-water lens extending approximately 40 units below MSL. The validity of the basic physical principle is frequently obscured by confusion between fresh-water inventory and actual potable

water. A 5 m lens of potable water will have the same head as a 10 m lens of 50% sea water, since the integrated density deficit of the water column is the same, even though salinity distributions and the potential utility of the water are radically different. In this paper, the term "fresh water" is used generically to indicate that fraction of the ground-water body which is attributable to rainfall recharge, regardless of the salinity of the total mixture.

It is generally recognized that there is not a sharp interface between fresh water and ocean water at the bottom of an island lens; various forces, especially tidal mixing, create a brackish transition zone. When this transition zone is considered, the depth to the 50% (sea water) isochlor is usually assumed to be equivalent to the depth of the idealized, unmixed fresh-water lens.

When we review the application of quantitative models to island ground-water systems, we note that there has been little systematic distinction between geologic types and origins of islands and their implications in terms of hydrogeology. In addition, a number of simplifying assumptions are usually applied to the models used. One of these is that there is a single, homogeneous aquifer; another is that tidal effects can be neglected. Another common set of assumptions is known as the Dupuit assumptions - that equipotential lines are vertical and that velocity is uniform over the depth of flow (Fetter, 1972). This implies strictly horizontal ground-water movement, and for a vertical cross-section reduces the problem to one space dimension.

The following conditions must exist, at least approximately, for the Dupuit assumptions to be valid: the fresh-water lens is thin compared to its lateral extent; the slope of the phreatic surface approaches horizontality;

thickness of the aquifer is much less than its lateral extent; the aquifer is underlain by an impermeable unit; and the interface between the saline and fresh water is distinct. In atoll island situations the first three of these conditions are typically met but, as will be discussed below, the last two are often wildly inappropriate.

Fetter (1972) used the Dupuit assumptions and ignored tidal effects in solving for the position of the saline-water interface beneath the South Fork of Long Island, New York. Comparing numerical and analytical calculations for the position of the interface, Fetter concluded that, "under natural conditions of fresh-water discharge", the error introduced by ignoring vertical flow components was negligible.

A water resources study of an atoll island (Tarawa) was performed by Lloyd et al. (1980). To simulate the lens configuration they used a finite difference approximation, assumed vertical components of flow to be negligible, and ignored tidal fluctuations. Although not considered, tidal-induced mixing was identified as a mechanism that would adversely affect correlation between calculated results and field observations. During simulation of periods of heavy rainfall, recharge to the lens was so high that calculated water level values rose above the land surface. It is possible that the assumption of only horizontal flow made adequate water movement through the aquifer impossible and caused unrealistic ground water accumulations in the simulation.

Fang et al. (1972) simulated two-dimensional (vertical plane), saturated ground-water flow in a coastal beach, using finite element analysis. They assigned a prescribed but fluctuating head at the shoreline, allowed flow across the bottom boundary of the surface aquifer, and assumed a single-density fluid. Although comparison of the water table calculations with field

data was good, their model solved for a free-water surface, and did not take into account unsaturated flow conditions.

The application of governing equations for a two-dimensional vertical plane, as well as tidal boundary conditions, was performed by Lam (1974) on Swains Island, in an attempt to devise a technique for assessing atoll aquifer permeabilities. He initially assumed the base of the surficial aquifer to be impermeable, the fluid to be of a single density, and provided a prescribed head ocean boundary that changed with time (simulating tidal fluctuations).

Based on recorded data for this atoll, phase lag (the difference between the time of high (or low) tide in the lagoon and the corresponding time of the ocean tide) was shown to be significant. Lam's original finite difference simulation failed, however, to adequately reproduce this lag relationship. In an effort to more closely approximate actual conditions, the model was modified to include small openings in the impermeable base to permit tidally driven flow to reach the surficial aquifer from below.

The significance of tidally driven ground-water flow at Enewetak Atoll, in the Marshall Islands, has been reported by Buddemeier and Holladay (1977), Buddemeier (1981), and Wheatcraft and Buddemeier (1981). Buddemeier and Holladay (1977) observed that on Enjebi Island tide lag decreased and tidal efficiency increased with increasing well depth. The authors hypothesized the existence of a more permeable carbonate unit beneath the surficial aquifer.

Further work on Enjebi Island by Wheatcraft and Buddemeier (1981) revealed that shallow well tide lags and amplitudes were independent of distance from the shoreline. It was noted that for large island and coastal aquifers, under conditions of horizontal signal propagation and horizontal ground-water flow, tidal signals decrease and phase lags increase with increasing distance from the ocean boundary (Ferris, 1951; Carr et al., 1969). Enjebi data were

compared to the standard horizontal flow conceptual model and to the results of an analytical model that also assumed horizontally propagated tidal signals. Neither model adequately simulated the field observations, suggesting that atoll island ground-water dynamics differ from large island and coastal conditions. The authors concluded that tidal signals are propagated vertically into the surface aquifer from a permeable lower aquifer, which they identified as the Pleistocene carbonate sequence found in coring operations at depths of 10-20 m below the present surface. Buddemeier (1981) showed that calculated sea-water residence times in the Pleistocene formation were consistent with, and may control, the fresh-water inventories observed on the various islands of Enewetak Atoll.

These observations are not consistent with the Dupuit assumptions and the conventional descriptions of Ghyben-Herzberg lenses in several important respects. The island aquifers are not hydrologically homogeneous, are not underlain by an impermeable base, and the vertical dimensions of the Pleistocene sections are in many locations large compared to horizontal reef or island dimensions. This means that vertical water flow and tidal mixing may be important features of atoll island fresh-water lenses, and that horizontal flow may not be assumed, nor tidal effects neglected.

Further, there is a large quantity of circumstantial evidence which indicates that these observations may be generalizable to other atoll and coral reef islands. Throughout the tectonically stable portions of the Indo-Pacific, the Holocene-Pleistocene contact under coral reefs typically occurs at depths of 7-25 m, and Pleistocene sediments show evidence of subaerial alteration during past episodes of lower sealevel. It is well established that exposed carbonate terrains commonly develop karst-like features (Vacher, 1978), and karsts are among the most permeable of sedimentary formations. The

cavernous and permeable nature of the carbonate substructure of reef systems has been documented by both drilling operations and hydrologic studies (Ladd and Schlanger, 1960; Jacobson and Hill, 1980; PRC Toups, 1983), and various writers have documented the karst-like topography of the antecedent structures underlying modern reefs (Hopley, 1982).

In view of these observations and their potential significance, a quantitative computer simulation was undertaken to test the validity and examine the implications of the layered aquifer model for atoll islands.

2. OBJECTIVES OF THE STUDY

The investigation reported in this paper was undertaken to develop a quantitative computer model of tidal signal propagation and water flow in a coral reef island consisting of a surficial Holocene aquifer overlying a more permeable Pleistocene aquifer connected hydraulically with the ocean and lagoon.

The primary goals of this effort were: (1) to assess the influence of tidal fluctuations upon atoll island ground-water dynamics; (2) to determine the significance of vertical ground-water flow; and (3) to test by comparison with field data for the hypothesized hydraulic connection between a surficial island aquifer and an underlying, more permeable, consolidated aquifer.

Because of the wealth of geologic and hydrologic data available for Enjebi Island, Enewetak Atoll, dimensions and hydrologic parameters appropriate to Enjebi were incorporated into the model in order to permit qualitative and quantitative comparisons of the computer simulation with observed field data.

Figure 1 shows the locations of Enewetak Atoll, Enjebi Island, and the test wells and transects discussed below.

3. METHODS AND MODEL PARAMETERS

Two major simplifying assumptions were made prior to selection and development of a quantitative model. First, it was decided to ignore fluid density differences resulting from salinity and/or temperature variations in the groundwater. This approach has been adopted by other workers (Fang et al., 1972; Lam, 1974), and after reviewing the relative potentials for flow induced by total head gradients and for that induced by density gradients in the Enjebi Island system, we concluded that tidal effects would dominate the system and, therefore, that a single-phase fluid flow model was acceptable.

Second, the system was modeled in a two-dimensional vertical plane normal to the longitudinal axis of the reef structure. Although this approximation is normally considered valid only for relatively symmetric "strip" islands with length \gg width, we consider it appropriate to Enjebi Island for three reasons: (1) as noted above, well tidal responses were essentially independent of well location, implying the absence of any edge effects on the surficial aquifer; (2) the underlying structure of the island, and particularly the Pleistocene aquifer, is not island-related but is a characteristic of the atoll reef structure, which is clearly a quasi-infinite strip formation; and (3) a smaller number of wells on Enewetak island (which clearly approximates the "strip island" structure) produced tidal responses similar in both magnitude and pattern to those on Enjebi. The model section through Enjebi Island is shown by the NE-SW line in Figure 1. The geologic section developed by Ristvet et al. (1978) is presented in Figure 2; although not coincident with the model section, it provides a qualitative representation of the formations modeled.

3.1 Numerical Solution Techniques

FEMWATER (Yeh and Ward, 1980) was chosen as the calculational tool for modeling this problem. FEMWATER employs the Galerkin finite element method, coupled with a finite difference time-marching routine, to solve the equations of transient, saturated-unsaturated ground-water flow in the two-dimensional vertical plane.

The five dependent variables for the problem are: pressure head (h); average velocity of the grains of the medium (\vec{v}_s); Darcy velocity of the fluid relative to the grains of the medium (\vec{q}_{fs}); fluid density (ρ_f); and moisture content (θ). Although fluid density eventually is treated as a constant in the model, it is initially treated as a variable to facilitate the derivation of the model equation for FEMWATER. Appendix 1 defines the symbols used for the scientific terms in the discussion which follows.

The five governing equations that are combined to describe flow through a saturated-unsaturated porous medium are (Yeh, 1982):

Continuity equation for a fluid

$$\frac{D}{Dt} \int_{V'}(t) \rho_f \theta dV = 0 \quad (1)$$

Continuity equation for a porous medium

$$\frac{D_s}{Dt} \int_{V'}(t) \rho_b (1-n_e) dV = 0 \quad (2)$$

Equation of fluid motion (Darcy's Law)

$$\vec{q}_{fs} = - \bar{K} \cdot \nabla H \quad (3)$$

Fluid compressibility equation

$$\rho_f = \rho_f^0 e^{\beta(p-p_0)} \quad (4)$$

Consolidation equation

$$(\lambda_s + 2\mu_s) \nabla^2 e^* = \nabla^2 \sigma \quad (5)$$

In addition to the above mentioned equations, specific moisture capacity was another important relationship used in the derivation of the FEMWATER equation. Step by step expansions of the governing equations can be found in Herman (1984).

Equations 1 through 5 are combined to form one equation for transient, simultaneous, saturated-unsaturated ground-water flow through a porous medium::

$$\left[\frac{d\theta}{dh} + \theta \beta \rho_f g + \frac{\theta}{n_e} \alpha \rho_f g \right] \frac{\partial h}{\partial t} = \nabla \cdot [\bar{K} \cdot (\nabla h + \nabla z)] \quad (6)$$

Equation 6 is based on the following assumptions: porous material is compressible, but individual grains are incompressible; bulk density of the medium is constant; changes in fluid density do not affect work done on the fluid by increases in pressure; pressure changes cause fluid density changes; for the unsaturated zone, changes in effective porosity with respect to pressure head are negligible; horizontal consolidation is negligible; and spatial changes in fluid density are negligible (Herman and Wheatcraft, 1984).

For an extremely detailed discussion of the finite element method, the

reader is referred to Zienkiewicz (1973). Application of the Galerkin method to the governing equations of FEMWATER is discussed in Reeves and Duguid (1975), Yeh and Ward (1980), and Yeh (1982).

3.2 Parameter Estimation

A data file of Enjebi hydrogeologic characteristics was used as input for the modified computer program. This file consisted of: (1) a set of dimensional values that define the finite element grid approximation of a vertical cross section through Enewetak Atoll; (2) a collection of physical parameters that describe the hydrogeologic conditions of the subsurface environment; and (3) a set of numerical values necessary to define the finite element topology.

A conceptual picture of the section modeled is shown in Figure 3, which identifies the major features and the model boundaries discussed below. The vertical boundary, located at the left side of the profile, was chosen arbitrarily in order to limit the grid size.

The cross section was divided into three horizontal hydrostratigraphic units: (1) volcanic basalt (depth = 1277 m); (2) consolidated limestone aquifer (Plio-Pleistocene to 200 m, Miocene and Eocene from 200 to 1277 m); and (3) surficial aquifer (Holocene, unconsolidated). Each aquifer was considered isotropic and homogeneous.

The finite element grid of the atoll cross section, both dimension and shape, was constructed from a topographic map of Enewetak Atoll and Vicinity (Emery et al., 1954). Figure 4 shows the portion of this grid corresponding to the surficial aquifer.

The consolidated aquifer was assumed to be saturated at all times, while the surficial unit was considered to be a phreatic aquifer. Characteristic

curves for the unsaturated portion of the upper aquifer were constructed from laboratory analyses of shallow Enjebi Island soils (Buddemeier, unpublished data). For both aquifers, the coefficient of compressibility of water (B) is $4.4 \times 10^{-10} \text{ m}^2 \text{ sec}^2/\text{kg m}$. Table 1 contains additional values for other hydrologic parameters.

Effective porosity (n_e) is based on data from Emery et al. (1954), and is probably accurate to within $\pm 50\%$ for the unconsolidated carbonate materials. However, in the Pleistocene aquifers the effective porosity may be considerably less for the well-cemented formations and may approach 100% for the cavernous voids.

The hydraulic conductivity of the surficial aquifer is based on determinations by Wheatcraft and Buddemeier (1981). Although natural variations are substantial, the value used agrees reasonably well with other data determined from well tests on surficial island aquifers (Jacobson and Hill, 1980; PRC Touns, 1984), and is almost certainly of the correct order of magnitude. The value used for the Pleistocene aquifer hydraulic conductivity was deliberately chosen to represent extreme, but not unreasonable, conditions; it is at the upper end of ranges of hydraulic conductivities given for karst formations by Freeze and Cherry (1979), and is approximately a factor of three greater than the highest reef and island hydraulic conductivities reported for shallow well tests (Oberdorfer and Buddemeier, 1983; Hunt, 1979). The intention was to test the model using the maximum credible permeability assumptions for the Pleistocene aquifer.

The tide signal used in the model was a sine wave with a twelve-hour period and a 1.8 meter amplitude; Enewetak tides are mixed semi-diurnal with a maximum (spring tide) range of 1.8 m. Lagoon and ocean tides were assumed to be in phase (see Buddemeier, 1981), and mean sea level was assumed to be the

same in both lagoon and ocean.

Both lagoon and ocean tide signals were assumed to be directly coupled to the Pleistocene formation. This approximation is probably valid for Enewetak, where the lagoon has a large number of pinnacle reefs which outcrop through the unconsolidated lagoon sediments. Recent seismic investigations have shown that the foundations of the pinnacles are almost certainly an extension of the Pleistocene formation (E. Shinn, personal communication); hence, the pinnacles can serve as pressure conduits to the underlying consolidated formation. Such an assumption may not be valid for lagoon systems which have thicker layers of Holocene sediments and fewer patch or pinnacle reefs.

3.3 Boundary Conditions and Calculation Procedures

For the initial conditions (time $t = 0$), every node in the finite element grid was assigned a pressure-head value based on the following equation:

$$h(x_i, z_i, 0) = 1277.0 - z_i \quad (7)$$

where the value 1277.0 represents mean sea level (in meters), measured from the consolidated aquifer's impermeable volcanic base; and z_i is the elevation head (vertical coordinate) of node "i".

The maximum elevation of the island is taken as 1280 m, so the 1277 m value for MSL corresponds to a depth of 3 m in Figures 4, 5, and 6. The first set of calculational nodes at a total depth of 4 m thus correspond to a depth of approximately 1 m below the water table. This is the approximate depth of the shallow test wells, the data from which are compared with the simulation results.

The boundaries B_1 and B_2 (Figure 3) were specified as modified Dirichlet

boundaries; that is to say, every node along these boundaries was assigned a new prescribed pressure-head value at the beginning of each time step, but the value remained constant throughout the time step. The right margin of boundary B_1 extends to a point on the surficial aquifer's land surface where lagoon high tide is marked. Correspondingly, the left margin of boundary B_2 extends to a point on the surficial aquifer's land surface where ocean high tide is marked. The equation used to express prescribed pressure head is

$$h(x_b, z_b, t) = 0.9 \sin(4\pi t/86400) + 1277.0 \quad (8)$$

where x_b and z_b are the spatial coordinates of any node located on boundaries B_1 or B_2 . Again, the above equation represents a mathematical approximation of the tide cycle for Enewetak Atoll. Numerical values have been substituted for previously discussed hydrologic parameters.

Boundary B_3 is a contact between the consolidated carbonate rock and the basalt volcano, while boundary B_5 is the island land surface above both ocean and lagoon high tides. Boundary B_4 was created to limit the grid size. All of these boundaries were treated as no-flow boundaries. Expressed mathematically,

$$q(x_c, z_c, t) = - \hat{n} \cdot [\bar{K} \cdot (\nabla h + \nabla z)] = 0 \quad (9)$$

where x_c and z_c are the spatial coordinates of any node located on boundaries B_3 , B_4 , or B_5 . This equation states that no water flux occurs across boundaries B_3 , B_4 , or B_5 .

Consecutive half-hour time steps were run until pseudo steady-state conditions were achieved, or in other words, when pressure distributions for

one time step were approximately the same as for a time step exactly 12 hours earlier. A simulated complete tide cycle occurs within a 12-hour period; therefore, "cycle steps" are defined as ranging from 0 to 12. For example, high tide corresponds to cycle step 3 and low tide corresponds to cycle step 9.

4. RESULTS

4.1 Tidal Efficiency and Lag Computations

Tidal efficiency and average tidal lag calculations were made for several rows of nodes within the upper aquifer as well as within the lower aquifer. These computations provided a means for analyzing the relation between lag and/or efficiency and depth and/or distance from a shoreline.

The orientation of depths and rows chosen for comparison appear in Figure 4. Not appearing in Figure 4 is a row of nodes at a maximum depth of 45 meters below land surface (42 m below MSL). This row was included in the analysis to serve as a representative sampling of nodes within the lower aquifer. The "distance from lagoon shoreline" nodal values are relative to the point on the shoreline where low tide is calculated to occur.

Nodal efficiency and tide lag values were calculated from simulated pressure-head results, and then plotted against distance from the lagoon shoreline (Figure 5). The results indicate that tidal efficiency increases and lag decreases with increasing depth. In the vertical sections underlying the intertidal zones, there is a relative decrease in the magnitude of the tidal signal as distance from either shoreline increases (Figures 4 and 5, sections A and C); however, the efficiency values in section B (underlying the supratidal portions of the island) do not tend toward zero, as would be the case when ground water flows in a principally horizontal direction.

The efficiencies and lags in section B remain quite constant with respect to horizontal distance, and values in the Pleistocene aquifer differ only marginally from the oceanic signal. This is a clear indication of vertical ground-water flow within the conceptual model's surficial aquifer. This observation, coupled with the fact that efficiencies increase with depth, proves that the conceptualization of a hydraulic connection between the actual surficial and consolidated aquifers is reasonable, and that the real-world consolidated aquifer exerts considerable control over the flow dynamics within the surficial aquifer.

The asymmetric shape of the lag and efficiency curves is due to the difference in land slope between the lagoon and ocean sides of the island. The island profile in Figure 4 shows that the land surface on the lagoon side possesses a much shallower slope than the land surface on the ocean side. Correspondingly, the nodal efficiency values for the lagoon side form a shallower slope than the ocean-side points. Relatively speaking, this relation suggests that the strength of the tidal signal decays more slowly on the lagoon side than on the ocean side.

4.2 Total Head Contour Maps

Total head contour maps of the aquifer cross section were constructed for the critical hours 0, 3, 6, and 9 (corresponding to rising, high, falling, and low tides, respectively); these are shown in Figure 6. The 12 hour sequence shown represents a complete tide cycle initiated on the 60th hour of simulation. For step 9, contour lines terminate at land surface, well above free standing water levels. This is because the nodes along the land surface, up to where the maximum high-tide levels occur, are prescribed-head nodes and therefore define where the contour lines should be plotted, independent of

head conditions within the aquifer.

Steps 0(12) and 3 represent water levels at mid-tide and high tide, and indicate that ground-water movement at the aquifer margins is directed from the ocean (or lagoon) inward. Beginning at the first time step, ground-water flow in the central portion of the aquifer is in an upward direction. This reflects the highly influential nature of the lower aquifer, as it relates to the ground-water flow system. As time progresses, the rising tide, via the lower aquifer, causes continued upward ground-water movement.

The geometry of the surficial aquifer is responsible for the asymmetric head responses displayed in the cross section. The steepness of the ocean-side slope, particularly in comparison to the lagoon-side slope, ensures that ground-water flow near the ocean boundary will be predominantly horizontal. This is evidenced by the almost vertical equipotential lines near the ocean and can be contrasted with the equipotential lines near the lagoon, which vary from vertical to being parallel to the land slope.

4.3 Velocity-Field Illustrations

Darcy-velocity fields (Figure 7) for the surficial aquifer were constructed for the same steps as the equipotential contours. These figures were qualitatively extrapolated from the total head contour maps, with the relative size of an arrow indicating the magnitude of the velocity.

The velocity fields of steps 3 (high tide) and 9 (low tide) very clearly reflect the effects that the tides have on ground-water flow. By the time high tide is reached, the ocean and lagoon have set up head gradients toward the interior of the surficial aquifer, while at low tide, ground water flows from the surficial aquifer toward the lower aquifer, lagoon, and ocean. In both cases (as well as for all other points in time), ocean and lagoon water-

level variations affect ground-water flow in the lower aquifer sooner than in the upper aquifer. This is due to the higher permeability of the lower aquifer, and is reflected in the lower tidal lags and higher efficiencies calculated for this aquifer. Water that is forced into the lower aquifer during a rising tide can only flow into the upper aquifer. More generally, all four velocity-field drawings serve to illustrate the dominant presence of vertical ground-water flow in the central portion of the island.

5. DISCUSSION

Before proceeding with a comparison of the field data and the computer simulation results, three important qualifications must be noted.

First, the major discrepancy between the model and the actual island is in the dimensions of the intertidal zones. While the total length of the island section is correct, the actual island beaches are stepped and/or bermed more steeply from the low-water mark. This results in intertidal zone dimensions of a few tens of meters at most, rather than the 135 m (oceanside) and 165 m (lagoon side) values adopted for the model. We proceeded on this basis for several reasons, the least noble being that it was considerably simpler to do so. However, an advantage gained was the better resolution of boundary effects and the factors controlling them; the pattern of variations seen in sections A and C of Figures 5, 6, and 7 would require modeling on a different scale if actual tidal zone dimensions were used. Finally, it should be noted that most of the shallow test wells which are the primary source of field data are far enough from the beach so that they do not fall into the spurious intertidal zone modeled.

The second point is that no effort was made to model any effects of the oceanward reef plate, which Ayers et al. (1984) have pointed out may act as a

leaky confining layer. At Enjebi, the reef plate only projects a short distance under the island (Figure 2), and reef drilling projects have demonstrated that the reef plate is only a rather thin veneer over unconsolidated and permeable sediments (Ladd and Schlanger, 1960; Oberdorfer and Buddemeier, 1983). In any event, perturbations would be limited primarily to the intertidal zone, and we consider neglect of reef plate effects justifiable in terms of the overall objectives of the study.

Finally, we note that the field data used for comparison come from two classes of wells. The shallow "1 m" wells were pits or piezometers which penetrated the water table 0.3-2.0 m and probably provide an accurate picture of water-table tidal responses. The deeper test wells were cased with continuously slotted casing, so tide signals are integrated over the entire depth and are more difficult to interpret (see Buddemeier and Holladay, 1977).

Figure 8 plots on a single figure both the field data and the computer simulation results for the surficial aquifer. Because of the geometry of Enjebi Island (Figure 1), some of the wells are closest to shorelines which are normal to the axis of the main reef, so all points were simply plotted as a function of distance from the nearest shoreline.

As noted above, both the shallow well field data and the simulation results for the central portion of the island are essentially independent of distance from shoreline. Furthermore, the numerical values for the actual "1 m" wells fall between the model values calculated for one meter and three meters below MSL in all cases except for those corresponding to the model's artificial intertidal zone.

We believe that the excellent qualitative and quantitative agreement between the simulation results and the field data not only demonstrates the validity of the two-layer aquifer model, but also validates our assumptions

about the magnitude of the Pleistocene aquifer hydraulic conductivity and effectiveness of its coupling to the lagoon and ocean tide signals.

In view of the success of this modeling effort, two further comments are warranted. First, from Figure 5 we see that the pattern of smooth change in efficiency across the intertidal zones is not matched by the pattern of lags (see especially the points around 200 and 800 m from the lagoon shoreline). This sheds some light on the persistent failure to find clean monotonic relationships between lag and efficiency in atoll island studies (Arnow, 1955; Ayers, 1984; Hunt and Peterson, 1980; PRC Touns, 1984). Clearly, the interaction of multiple pathways for the tide signal can result in locally variable relationships between lag and efficiency, and such variability may be diagnostic of the presence of multiple aquifer systems.

Finally, the results of this study bear on a local phenomenon on Enjebi Island. Well XEN-1 (Figure 2) is very close to the ocean shoreline, deep, and has a very short lag and moderately high efficiency, yet it has a large freshwater inventory and a very stable structure of salinity reductions at depth (Noshkin et al. 1976; Buddemeier and Holladay, 1977). Reference to Figures 6 and 7 suggests that the hydraulic and geometric factors at this location may result in very little net lateral displacement of water, permitting the vertical mixing to sustain reduced salinities to a substantial depth in the formation.

6. CONCLUSIONS

Based on the results of this computer simulation and its comparison to field studies, we conclude that:

A. Computer modeling of atoll island ground-water systems can be a

valuable interpretive and predictive tool if it is based on an adequate conceptual model and supported by the necessary data.

B. At Enewetak Atoll, island hydrology is controlled by a layered aquifer system consisting of an unconsolidated Holocene aquifer supported by a highly permeable Pleistocene aquifer. Specific conclusions derived from this are:

1. Vertical water movement predominates throughout most of the surficial aquifer;
2. The Pleistocene aquifer has hydraulic conductivity on the order of 10^3 m/day; and
3. Lagoon and ocean influences on the island ground water are affected primarily via the lower aquifer, rather than horizontally through the surficial aquifer.

C. The available literature on atoll geology and hydrology suggests similar effects may be expected in many, if not most, atoll islands. This implies that the traditional approach of modeling a classic Ghyben-Herzberg lens using the Dupuit assumptions may be inappropriate in many cases.

APPENDIX 1 - LIST OF SCIENTIFIC TERMS

<u>Symbol</u>	<u>Definition</u>	<u>Dimensions</u>
e^*	Dilation of the medium	Dimensionless
g	Acceleration of gravity	(L/T^2)
h	Pressure head	(L)
H	Hydraulic (total) head	(L)
\bar{R}	Hydraulic conductivity tensor	(L/T)
\hat{n}	Unit normal vector	Dimensionless
n_e	Effective porosity	Dimensionless
p	Fluid pressure	(M/LT^2)
p_0	Datum fluid pressure	(M/LT^2)
q	Darcy velocity of the fluid	(L/T)
\vec{q}_{fs}	Darcy velocity of the fluid relative to the grains of the medium	(L/T)
t	Time	(T)
\vec{v}_s	Average velocity of the grains of the medium	(L/T)
V	Volume	(L^3)
$V'(t)$	"Dummy" limit of integration	(L^3)
z	Vertical component of direction, or the elevation head	(L)
α	Coefficient of compressibility of water	(L^2T^2/ML)
β	Coefficient of compressibility of water	(L^2T^2/ML)
θ	S_{n_e} = moisture content	Dimensionless
λ_s	Lame's elastic constant	(ML/L^2T^2)
μ_s	Lame's shear modulus	(ML/L^2T^2)

<u>Symbol</u>	<u>Definition</u>	<u>Dimensions</u>
ρ_b	Bulk density of the medium	(M/L ³)
ρ_f	Fluid density	(M/L ³)
ρ_f^0	Fluid density at datum pressure	(M/L ³)
σ	Incremental fluid pressure	(M/LT ²)
dV	Differential volume element at $t > 0$	(L ³)
∇	Differential vector operator	(1/L)
$\frac{D}{Dt}$	Material derivative with respect to the average velocity of the fluid	(1/T)
$\frac{D_s}{Dt}$	Material derivative with respect to the average velocity of the solids	(1/T)

REFERENCES

Arnow, T., 1955. The Hydrology of Arno Atoll. Atoll Res. Bull. 44: 1-15.

Ayers, J. F., Vacher, H. L., Clayhulte, J. N., Stout, D., and Stebrinsky, R., 1984. Hydrogeology of Deke Island, Pingelap Atoll, Eastern Caroline Islands. Technical Report No. 52, Water and Energy Research Institute of the Western Pacific, University of Guam.

Buddemeier, R. W., 1981. The Geohydrology of Enewetak Atoll Islands and Reefs. In: Vol. 1, Proceedings Fourth International Coral Reef Symposium. Marine Sciences Center, University of Manila, Phillippines, pp. 339-345.

Buddemeier, R. W., and Holladay, G., 1977. Atoll Hydrology: Island Groundwater Characteristics and their Relationship to Diagenesis. In: Vol. 2, Proceedings Third International Coral Reef Symposium, University of Miami. Miami, Florida, pp. 167-173.

Carr, P. A., and Van Der Kamp, G. S., 1969. Determining Aquifer Characteristics by the Tidal Method. Water Resour. Res., 5(5): 1023-1031.

Emery, K. O., Tracy, J. I., and Ladd, H. S., 1954. Geology of Bikini and Nearby Atolls. U.S. Geol. Survey Prof. Paper 260-A.

Fang, C. S., Wang, S. N., and Harrison, W., 1972. Groundwater Flow in a Sandy Tidal Beach, 2. Two-Dimensional Finite Element Analysis. Water Resour. Res., 8(1): 121-128.

Ferris, J. G., 1951. Cyclic Fluctuations of Water Level as a Basis for Determining Aquifer Transmissibility. Assemblee Generale de Bruxelles, Assoc.

Int. d'Hydrologic Scientifique, 2: 148-155.

Fetter, C. W., Jr., 1972. Position of the Saline Water Interface Beneath Oceanic Islands. Water Resour. Res., 8(5): 1307-1315.

Freeze, R. A., and Cherry, J. A., 1979. Groundwater. Prentice-Hall, Inc., Englewood Cliffs, New Jersey. 604 pp.

Herman, M. E., 1984. Tidal Fluctuations and Ground-Water Dynamics in Atoll Island Aquifers. Masters Thesis, University of Nevada-Reno.

Herman, M. E., and Wheatcraft, S. W., 1984. Groundwater Dynamics Investigation of Enjebi Island, Enewetak Atoll: An Interpretive Computer Model Simulation. In: Proceedings of the 5th International Conference on Finite Elements in Water Resources. Burlington, Vermont, pp. 133-142.

Hopley, D. The Geomorphology of the Great Barrier Reef: Quaternary Development of Coral Reefs. Wiley Interscience, New York, 1982. 453 pp.

Hunt, B., 1979. An Analysis of Groundwater Resources of Tongatopee Island, Kingdom of Tonga. J. Hydrol. 40: 185-196.

Hunt, C. D., and Peterson, F. L., 1980. Groundwater Resources of Kwajalein Island, Marshall Islands. Water Resources Research Center Tech. Report No. 126, University of Hawaii, Honolulu.

Jacobson, G., and Hill, P. J., 1980. Groundwater Resources of Niue Island. BMR Record 1980/14, Bureau of Mineral Resources, Geology and Geophysics, Department of National Development, Canberra, Australia.

Ladd, H. S., and Schlanger, S. O., 1960. Drilling Operations on Enewetak Atoll. USGS Prof. Paper 260-Y, U.S. Government Printing Office, Washington, D.C.

Lam, R. K., 1974. Atoll Permeability Calculated from Tidal Diffusion. J. Geophys. Res., 79(21): 3073-3081, July.

Lloyd, J. W., Miles, J. C., Chessman, G. R., and Bugg, S. F., 1980. A Groundwater Resources Study of a Pacific Ocean Atoll - Tarawa, Gilbert Islands. Water Resour. Bull., Am. Water Res. Assoc., 16(4): 646-653, Aug.

Noshkin, V. E., Wong, K. M., Marsh, K., Eagle, R., Holladay, G., and Buddemeier, R. W., 1976. Plutonium Radionuclides in the Groundwater at Enewetak Atoll. In: Transuranium Nuclides in the Environment, Int. Atomic Energy Agency, Vienna, pp. 517-543.

Oberdorfer, J. A., and Buddemeier, R. W., 1983. Hydrogeology of a Great Barrier Reef: Implications for Groundwater in Reef and Atoll Islands. EOS 64: 703.

PRC Toups, 1983. Final Engineering Study to Evaluate Potable Water Supply Alternatives and Groundwater Yield at Diego Garcia, BIOT. Report to U.S. Naval Facilities Engineering Command, Pacific Division, by PRC Toups, Orange, California.

Reeves, M., and Duguid, J. O., 1975. Water Movement Through Saturated-Unsaturated Porous Media: A Finite Element Galerkin Model. Rep. ORNL-4927. Oak Ridge National Laboratory, Oak Ridge, Tenn., 232 pp.

Ristvet, B. L., Tremba, E. L., Couch, R. F., Fetzer, J. A., Goter, E. R., Walter, D. R., and Wendland, V. P., 1978. Geologic and Geophysical Investigations of the Enewetak Nuclear Craters. U.S. Air Force Weapons Laboratory Report AFWL-TR-77-242. Kirtland Air Force Base, NM.

Vacher, H. L., 1978. Hydrogeology of Bermuda - Significance of an Across-the-Island Variation in Permeability. J. Hydrology 39: 207-226.

Wheatcraft, S. W., and Buddemeier, R. W., 1981. Atoll Island Hydrology. Ground Water, 19(3): 311-320, May-June.

Yeh, G. T., and Ward, D. S., 1980. FEMWATER: A Finite Element Model of Water Flow Through Saturated-Unsaturated Porous Media. Rep. ORNL-5567. Oak Ridge National Laboratory, Oak Ridge, Tenn., 153 pp.

Yeh, G. T., 1982. Training Course No. 1: The Implementation of FEMWATER (ORNL-5567) Computer Program Final Report. Rep. ORNL/TM-8327. Oak Ridge National Laboratory, Oak Ridge, Tenn., 117 pp.

Zienkiewicz, O.C., 1973. The Finite Element Method in Engineering Science. McGraw-Hill (England), 1971.

This work was performed under the auspices of the U.S. Department of Energy by Lawrence Livermore National Laboratory under contract No. W-7405-Eng-48.

DISCLAIMER

This document was prepared as an account of work sponsored by an agency of the United States Government. Neither the United States Government nor the University of California nor any of their employees, makes any warranty, express or implied, or assumes any legal liability or responsibility for the accuracy, completeness, or usefulness of any information, apparatus, product, or process disclosed, or represents that its use would not infringe privately owned rights. Reference herein to any specific commercial products, process, or service by trade name, trademark, manufacturer, or otherwise, does not necessarily constitute or imply its endorsement, recommendation, or favoring by the United States Government or the University of California. The views and opinions of authors expressed herein do not necessarily state or reflect those of the United States Government thereof, and shall not be used for advertising or product endorsement purposes.

Table 1. Relevant Hydrologic Parameters

Aquifer	B (m ² sec ² /kg m)	n _e	K _{xx} (m/sec)	K _{zz} (m/sec)
Surficial	1.0E-08	0.30	0.69E-03	0.69E-03
Consolidated	1.0E-09	0.30	0.69E-01	0.69E-01

FIGURE CAPTIONS

- Figure 1. a) Enewetak Atoll, showing location of Enjebi Island.
b) Enjebi Island, showing locations of test wells, computer simulation transect (-), and geologic section transect (- - -; see Figure 2).
- Figure 2. Geologic cross section of Enjebi Island (Ristvet et al., 1978). See Figure 1 for section location.
- Figure 3. Conceptual model of the atoll section through Enjebi Island used for computer simulation. B₁-B₅ represent the model boundaries discussed in the text.
- Figure 4. Finite element grid of surficial aquifer cross section, Enjebi Island. Calculational nodes in the lower aquifer are not shown. Sections A and C correspond to the simulated intertidal zones, B to the central (supratidal) portion of the island.
- Figure 5. Calculated aquifer tide signal responses as a function of depth and distance from shoreline. Ocean shoreline is 945 m from lagoon shoreline; sections A-C are as defined in Figure 4. (a) Tide lag in hours. (b) Tidal efficiency relative to ocean tide.
- Figure 6. Total head contour maps for Enjebi Island model section. Contour interval = 0.1 m; MSL = 1277.0 m. Time after beginning of simulation: a) 60 hours (rising tide); b) 63 hours (high tide); c) 66 hours (falling tide); d) 69 hours (low tide).
- Figure 7. Velocity field maps for the model section of the surficial aquifers, Enjebi Island. Scales and tide cycle steps are the same as for Figure 6. Velocities are uncalibrated, but proportional to vector lengths.
- Figure 8. Comparison on observed and calculated aquifer tide responses as a function of depth and distance from shoreline. The region to the left of the labeled vertical line corresponds to the simulated intertidal zone; the actual intertidal is ≤ 50 m. (a) Tidal efficiency. (b) Tidal lag.

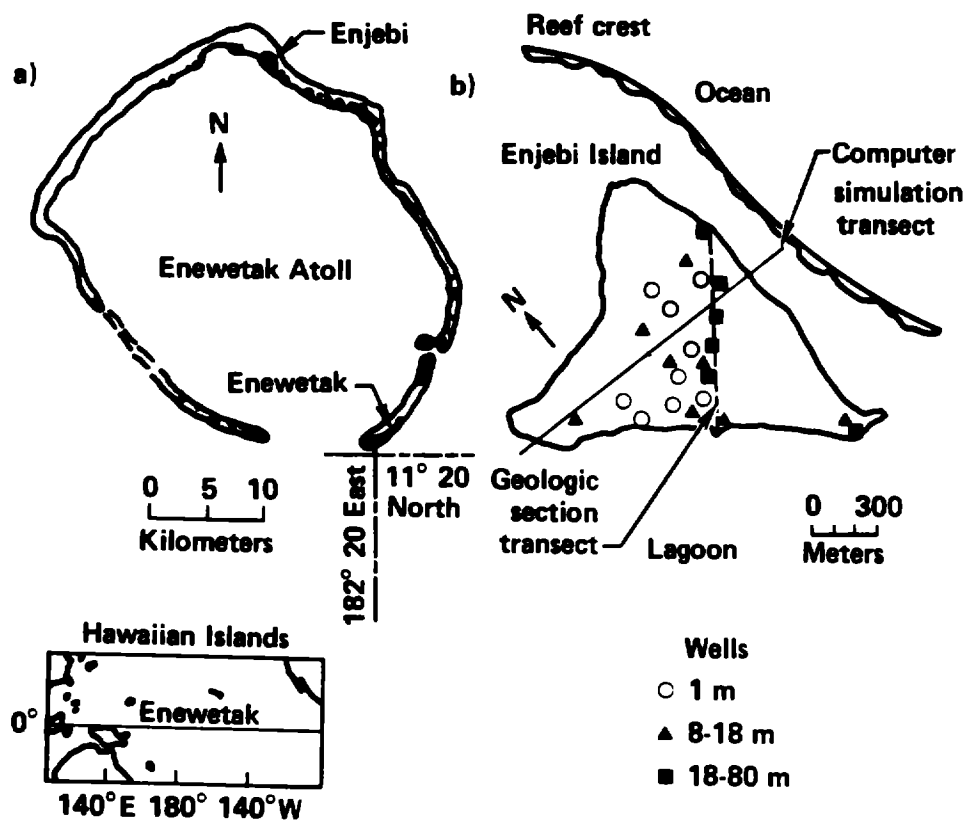


FIGURE 1

Herman, et al.

"A Layered Aquifer Model..."

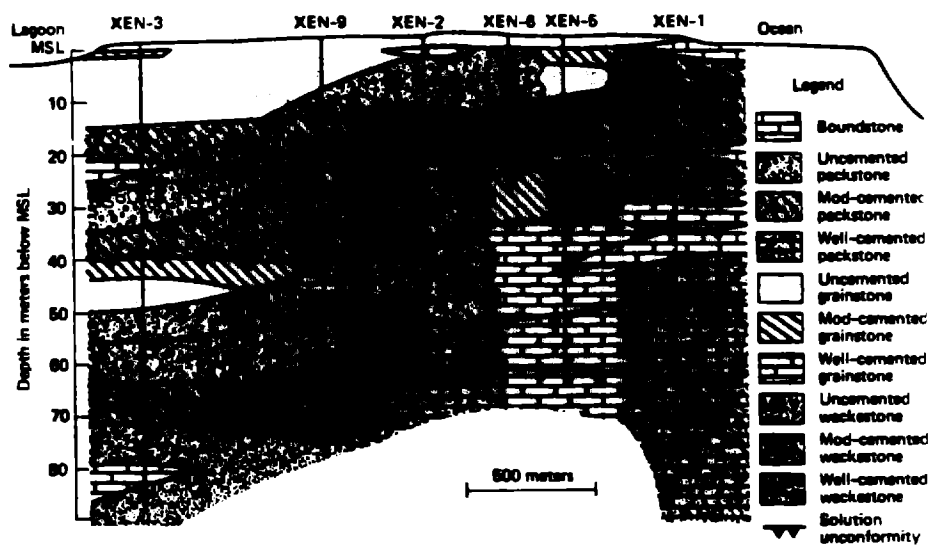


FIGURE 2
Herman, et al.
"A Layered Aquifer Model..."

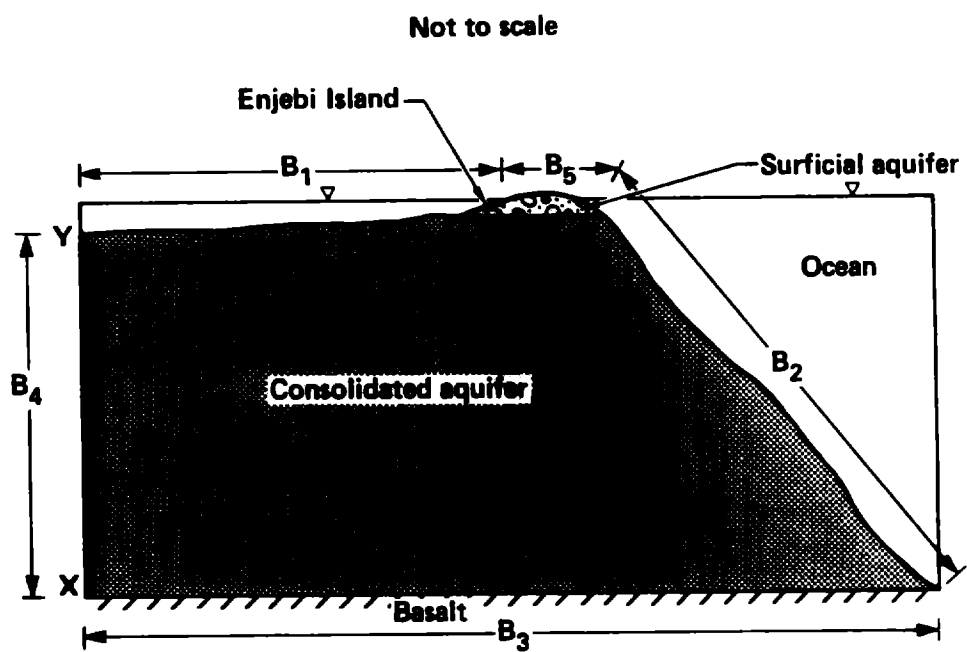


FIGURE 3

Herman, et al.

"A Layered Aquifer Model..."

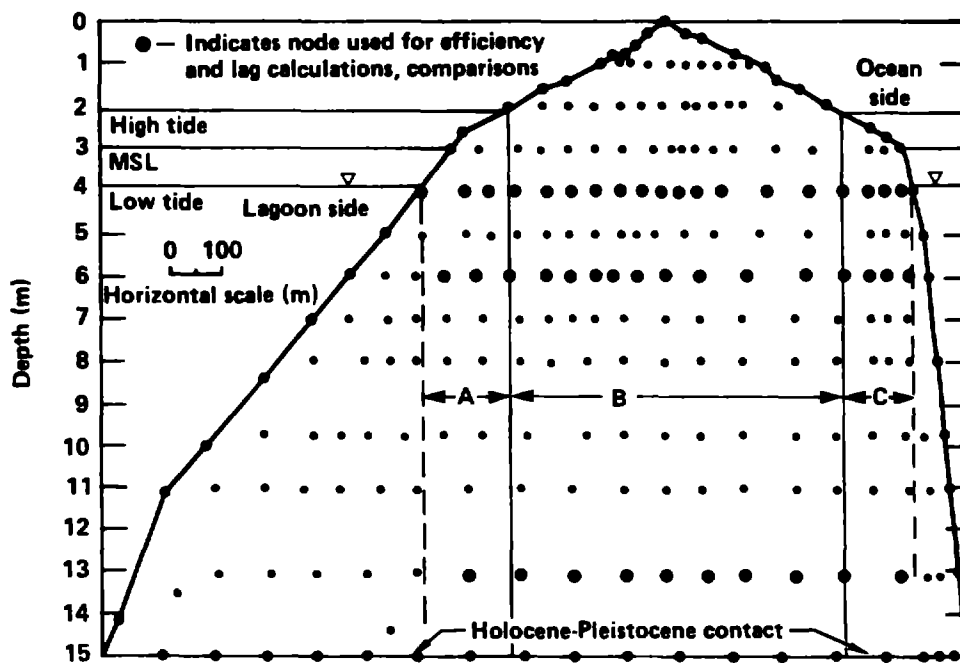


FIGURE 4
Herman, et al.
"A Layered Aquifer Model..."

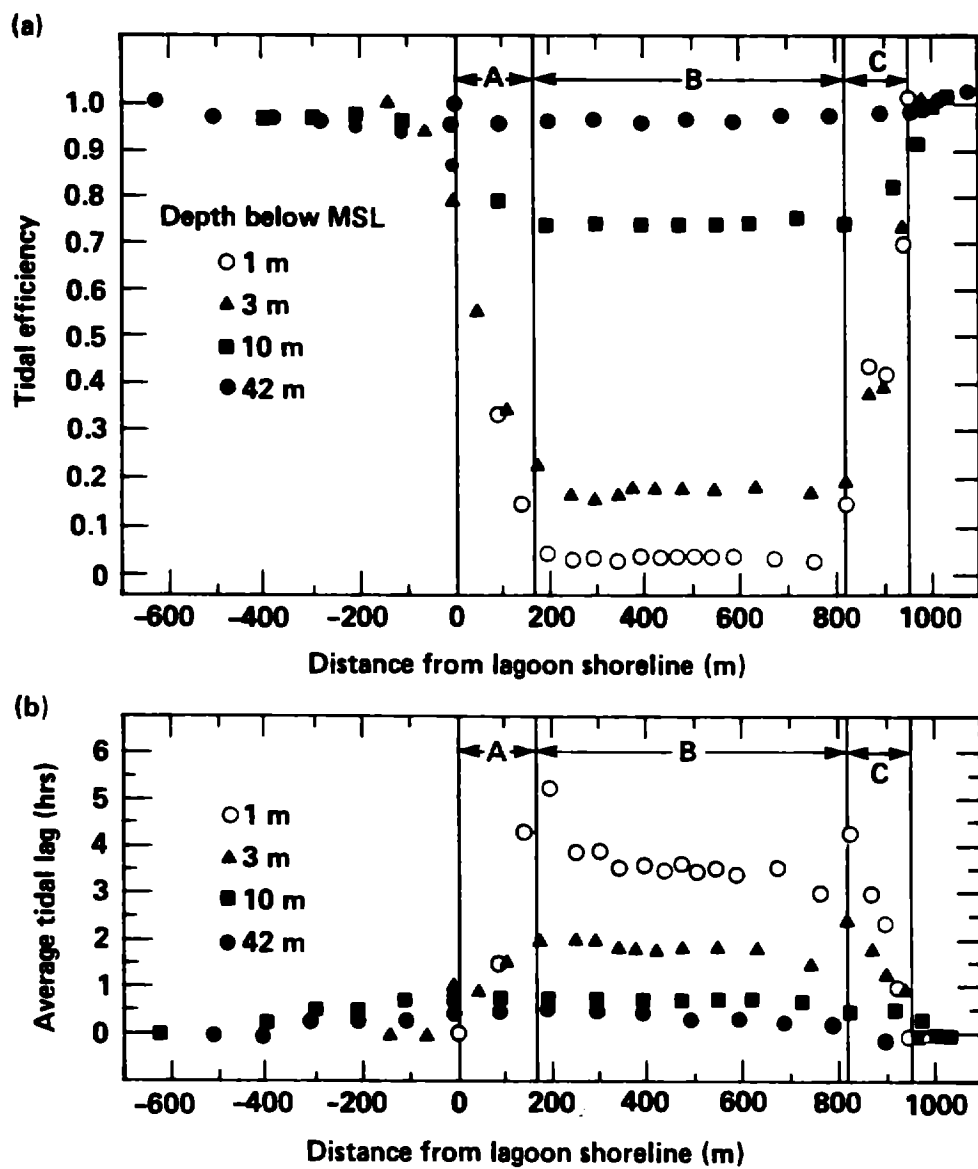


FIGURE 5

Herman, et al.

"A Layered Aquifer Model..."

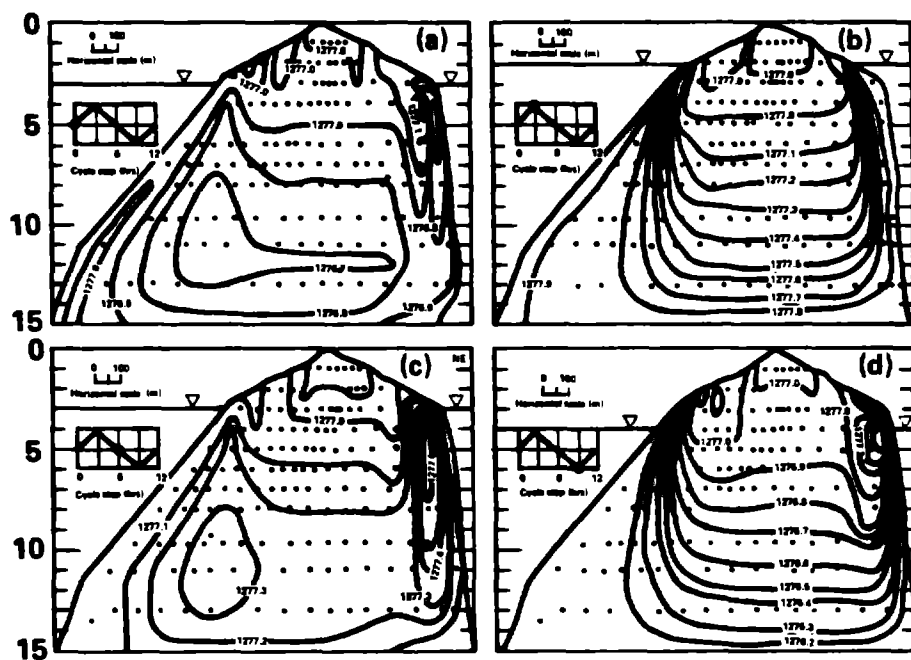


FIGURE 6
Herman, et al.
"A Layered Aquifer Model..."

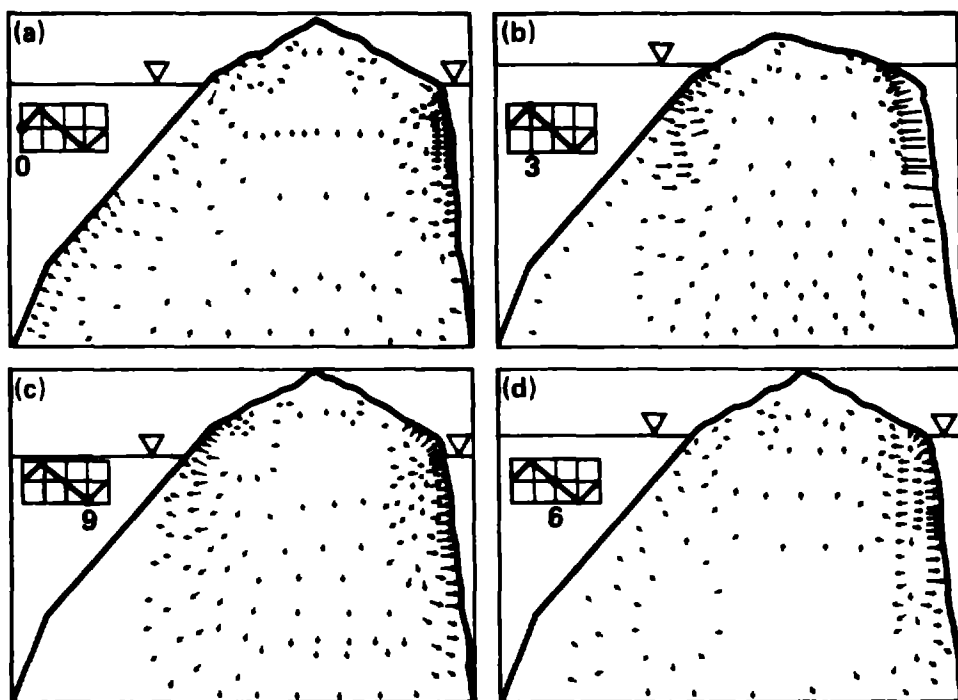


FIGURE 7
Herman, et al.
"A Layered Aquifer Model..."

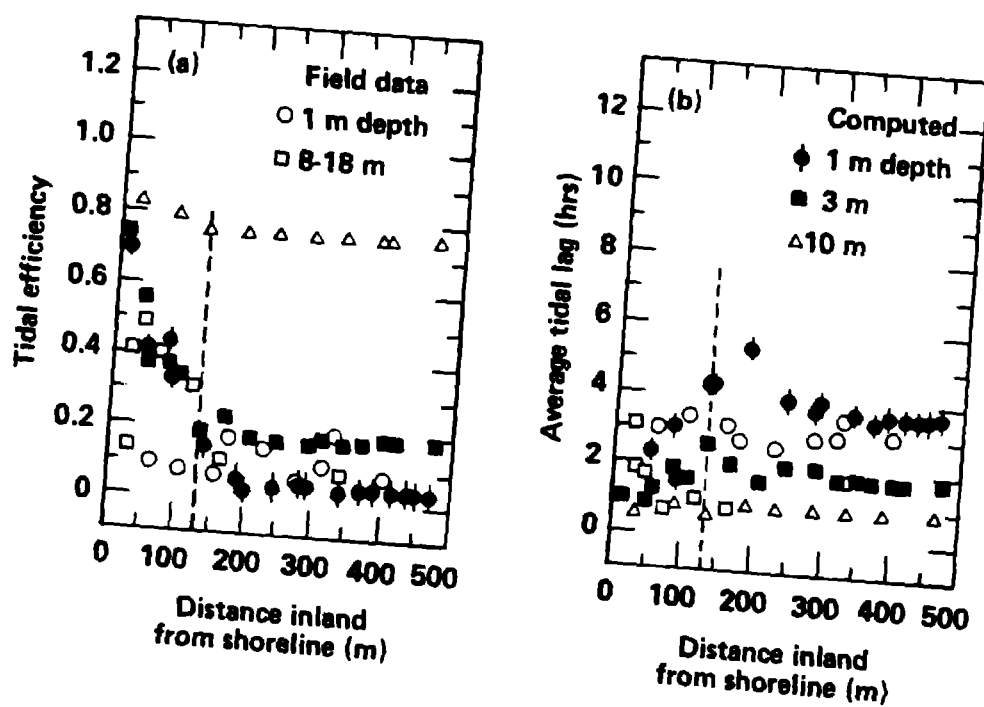


FIGURE 8
Herman, et al.
"A Layered Aquifer Model..."